Chapter 4 Results and Discussions

The vapor phase deposition is a simple process in which condensed source materials are vaporized at elevating temperature and then the resultant vapor phase condensed under certain conditions (temperature, atmosphere, pressure, substrate, *etc*) to synthesize the prospective products. As expected, fairly oriented single-crystalline hexagonal ZnO tetrapods had grown onto the substrates *via* a vapor-solid (VS) process in the work. Under controlling conditions, the ZnO tetrapods with higher aspect ratios were synthesized. In this chapter, we present the results of experiment—the effects of growth ambience of ZnO tetrapods, the emission properties relating to morphology, and the possible growth mechanisms of oriented ZnO structures

Most of ZnO tetrapods were synthesized at the distance 60 mm from the Zn vapor source. It approximately equals to two-third position of total length for the bottom tube to open-end, as shown in Fig. 4.1.

4.1 The Effects of Growth Ambience of ZnO Tetrapods

4.1.1 The air atmosphere

Figure 4.2 shows the SEM and TEM micrographs of the ZnO tetrapods resulting from the vapor phase deposition carried out in air atmosphere. Large area of ZnO tetrapods were formed by homogeneous nucleation and growth without the existence catalyst. The SEM images of tilted sample reveal that most of the nanostructures are highly oriented. The bright-field (BF) of TEM micrograph of single ZnO tetrapods and selected-area electron diffraction (SAED) pattern show the nanorod was a single crystal. The ZnO tetrapods grown on silicon substrate at the same condition are illustrated in Fig. 4.3. The diameters of the tetrapods are ranging from 100 nm to 1 μm and their lengths are 1 to 30 μm.

4.1.2 The H_2O atmosphere

The shape of ZnO tetrapods grown in H_2O ambience is more uniform than that in air atmosphere, as shown in fig. 4.4.

The lengths of ZnO tetrapods are in the range of 4-5 μm and diameters about 500 nm as revealed by SEM micrographs. The BF image of single ZnO tetrapods and the SAED pattern show that the ZnO nanorod is a single crystal. Figure 4.5 presents uniform shape for armor-unit like ZnO tetrapods. Similar results were also reported by Yang's *et al.* [11], but there was no O_2/Ar mixture flow employed in our experiment. This result suggested that oxygen concentration in the ambience affects the morphology of ZnO tetrapod. Furthermore, the ZnO tetrapods synthesized in air condition can be found in H_2O condition.

4.1.3 The H_2O_2 atmosphere

The ZnO tetrapods exhibited very different morphologies in the H_2O_2 atmosphere. Figure 4.6 shows the aggregated ZnO tetrapods synthesized on silicon. The ZnO tetrapods had lengths of 3 - 6 μm and diameters of 200 nm - 2 μm. Furthermore, the trumpet-shaped ZnO tetrapods shown in Fig. 4.6**c** have been reported in Yang *et al.* [11]. The ZnO tetrapods exhibit a bat-shape with hexagonal end-point of rod at the far side of the sample, as shown in Fig. 4.7. Moreover, more bottle-shaped ZnO tetrapods produced large yield in the rim region for the sample show in Fig. 4.8. They are all tetrapod like but with different shape. Hence, the tetrapods shape is largely affected by the oxygen concentration of reaction atmosphere. In high oxygen atmosphere, tetrapods grew not only along the [0001] direction but also toward the basal plane growth. As discussed by Z. L. Wang [50], the [0001] is the typical growth direction of one-dimensional ZnO nanostructures. Our work indicated that in rich oxygen atmosphere the tetrapods grow not only $\vec{c}$-axis but along the basal plane direction. The Yang *et al*. study[11], they varied the ratio of O_2/Ar gas flow from o.5-5% to 5-10% to cause the morphology of tetrapods changes from armor-unit-shape to trumpet-shape, and the end of tetrapods arm grew coarser and bigger. Their results are very the same as ours. The morphology of ZnO structures would be synthesized variously in different rich oxygen region. Tetrapods even turn into multi-rods in richer oxygen region as shown in Fig. 4.9. In Djurisic work [47], multi-pod structures had been observed by employed the ZnO: C: GeO_2 (1:1:0.1) mixture at 1100°C. Consequently, the activity energy barrier of tetrapod nucleation is lower than other morphology of ZnO crystals. Equally important, the ZnO tetrapods synthesized in H_2O condition can be found in H_2O_2 condition. Finally, we propose a schematic chart of the ZnO tetrapods nucleation and growth state, as illustrated in Fig. 4.10.

4.2 The CL and PL spectra of ZnO Tetrapods

Cathodoluminescence (CL) and Photoluminescence (PL) characterization of ZnO tetrapod grown in three experimental conditions is presented in this section. As shown in Fig. 4.11, the tetrapods synthesized in air atmosphere exhibit a UV band at 380 nm and a green band at 520 nm. Similar results have also been reported in Roy and Djurisic [46]. In their dopant-free samples, the luminescence spectra showed a characteristic UV emission and broad green emission, as shown in Fig. 2.11. The CL detected stronger UV emission and broad green emission in our experiment for the specimens grown in air atmosphere, which is poor oxygen concentration in comparison with the atmospheres in H_2O or H_2O_2. The ZnO tetrapods synthesized in poor oxygen concentration might be more crystalline, so that CL spectra of tetrapods exhibited stronger UV emission and broad green emission. On the other hand, the CL spectra show the weak UV emission and broad green emission from specimen grown in H_2O atmosphere (Fig. 4.12).

The CL spectra show only green emission for the specimens grown in H_2O_2 condition, as shown in Figs. 4.13 and 4.14. In this condition, the partial oxygen pressure in H_2O_2 equal to 0.8386 atm, it’s greater than the partial oxygen pressure in H_2O (4.6837×10^{-6} atm) and in air ambience (0.21 atm). Even though the morphologies of ZnO crystals are different, their CL spectra are similar. As discussed early in section 2.3, B. D. Yao reported that nanowires—synthesized by using ZnO source at 500-650^{o}C— with 200 nm in diameter exhibited the UV emission and stronger green emission [26], but the nanowires—synthesized by using ZnO source at 925^{o}C— with 222 nm in diameter also exhibited stronger

UV emission and broad green emission [48]. Similar morphologies are synthesized in different growth temperature could result different emitted properties. However, different morphologies of ZnO crystals exhibited similar emitted properties in our experiments, as shown in Figs. 4.13 and 4.14. Hence the emission properties of ZnO crystal do not relate to its morphology. Unambiguously, the microstructure of ZnO crystal should dominate the emission properties. The oxygen content in the ZnO crystal changes the defects, such as lattice packed (lattice constant) mismatch, so that the energy band gap varied and the emission properties of ZnO crystal change.

ZnO tetrapods synthesized in three ambiences exhibited different PL spectra, as shown in Fig. 4.15

4.3 Crystal Growth and Mechanisms of Oriented ZnO Structures

Pyramid growth hypothesis is proposed to the mechanism of nucleation and growth of ZnO tetrapod in this work, as shown in Fig. 4.16. This model illustrates the orientation relationship and the measured angle between each rod which agreed exactly with the calculation for tetrahedral model, and each angle between every two rod is 109^{o} as presented in Fig. 4.17.

For tetrapod growth, ZnO nuclei formed in the quartz tube *via* homogeneous nucleation in gas phase. Firstly, zinc vapor and oxygen vapor combined to form the vapor clusters. Clusters adhered to each other to decrease the surface energy, and liberated the latent heat during the solidification process. The lower temperature nuclei kept growing up as higher temperature ZnO vapor cluster adhered. Then, according to the rigid body rotation and collision in space, ZnO nuclei grew to tetrahedral pyramid configuration and grew far away from the direction center of pyramid structure. Finally, the tetrapod configuration of single-crystalline ZnO was synthesized to form “armor unit” shape. The definition of tetrapod nanorod comes from the geometrical similarity to the armor unit that it is used as primary wave protection.

A HR-TEM image of the top view is shown in Fig. 4.18. These bright-field images show that the entire nanorod is a complete single-crystalline, and reveals that the ZnO nanorods are single crystal with the growth direction perpendicular to the (0001) lattice planes. Many clusters distributive adhered on the surface of each rod are the direct evidence to the nanostructures of ZnO synthesized by the VS growth mechanism in vapor deposition, as discussed early in Z. L. Wang [34, 50]. Apparently, each lattice of individual cluster is match to the lattice of inter-rod. Clusters aggregated to contribute toward the lattices grown, and then the parallel lattices grew at a radial direction of [0001] to form the individual rod by layer-by layer growth. This model presented here can be adopted explain the helical growth mechanism as mentioned in Ch2 [34]. The anisotropic growth was due to the prefer orientation for ZnO constructure. Undoubtedly, the growth mechanism of rods followed helical like growth as presented in Fig.4.19. Obviously, the growth model of rods grew loop-by-loop with symmetric toward one direction of center axis.

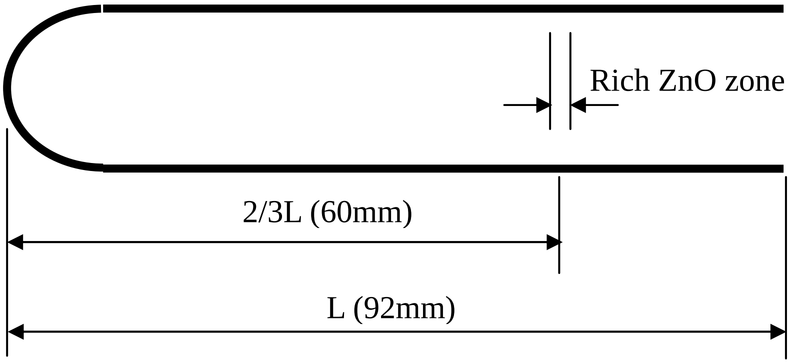

Figure 4.1 A illustration for the region of rich ZnO synthesized.

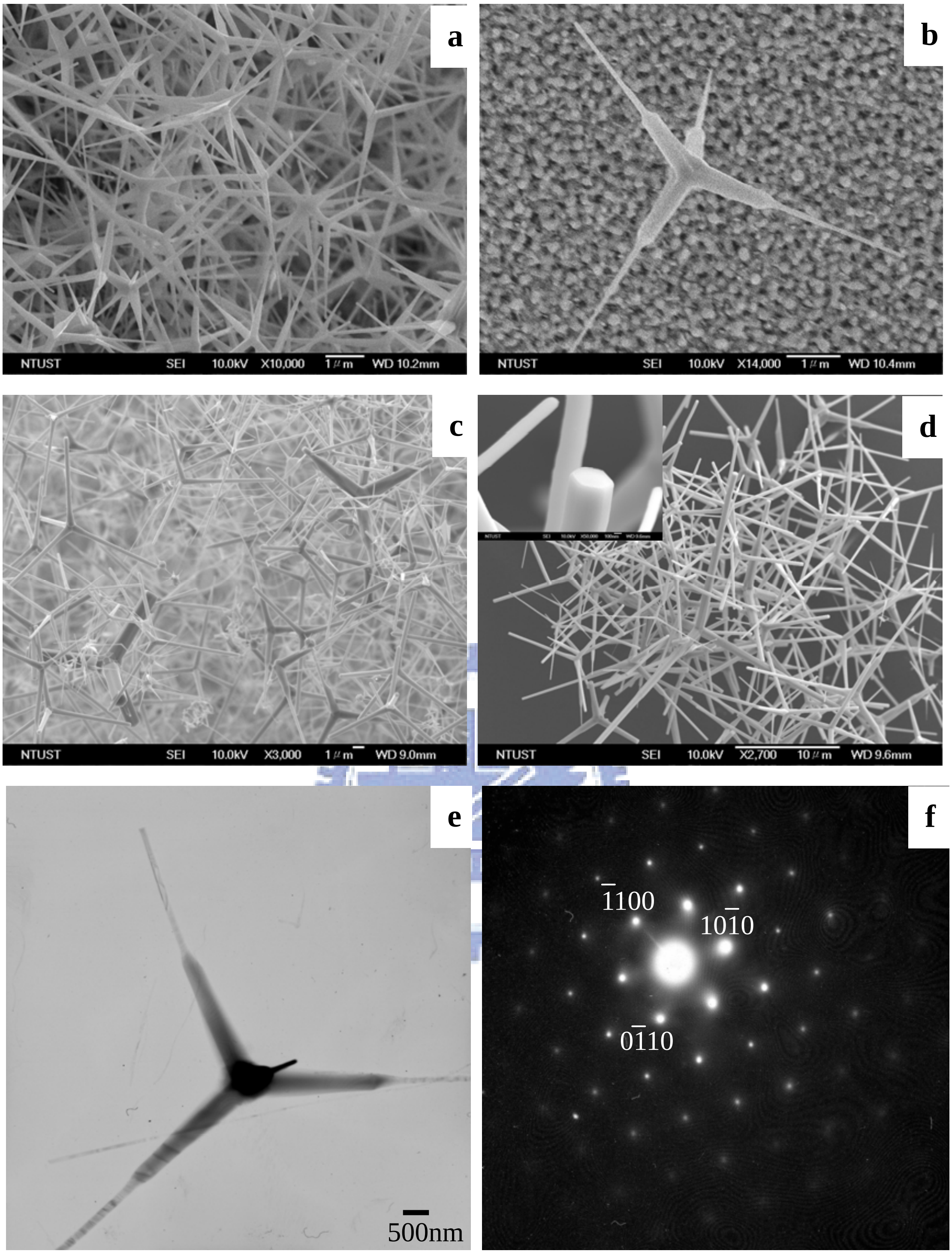

Figure 4.2 Micrographs of ZnO tetrapods grown on AAM substrate by vapor-phase-deposition at 950°C for 10 min in air atmosphere. **a**) Aggregated ZnO tetrapods. **b**) A tilted view image of a freestanding single-crystalline ZnO tetrapod. **c**) Face-on view image of the aggregated ZnO tetrapods. **d**) High magnification image of the aggregated ZnO tetrapods. Inset in Fig. 4.2**d** presented hexagonal shape for the end-point of tetrapod. **e**) A bright-field TEM image of the single ZnO tetrapods. f) A [0001] zone-axis selected-area electron diffraction (SAED) pattern of Fig. 4.2**e**.

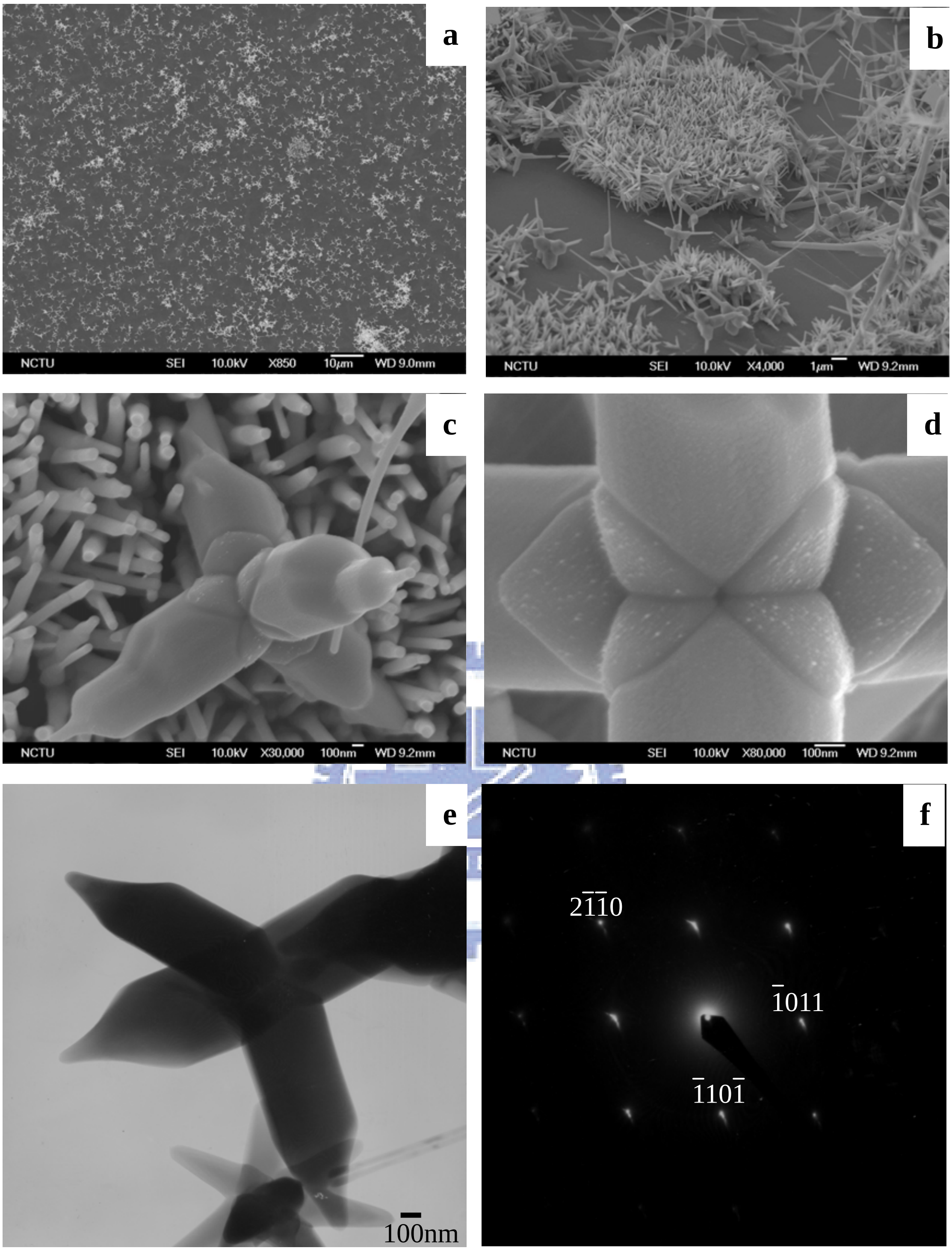

Figure 4.3 Micrographs of T-ZnO nanorods grown on silicon substrate by vapor-phase-deposition at 950^{o}C for 10min in air atmosphere. **a**) Low magnification, top view image of the sample. **b**) Tilted view image of the sample. **c**) Face-on view image of the single ZnO tetrapod. **d**) High magnification, bottom view image of the single ZnO tetrapod. **e**) A bright-field TEM micrograph of the single ZnO tetrapod. **f**) A $[01\bar{1}1]$ zone-axis selected-area electron diffraction (SAED) pattern of Fig. 4.3**e**.

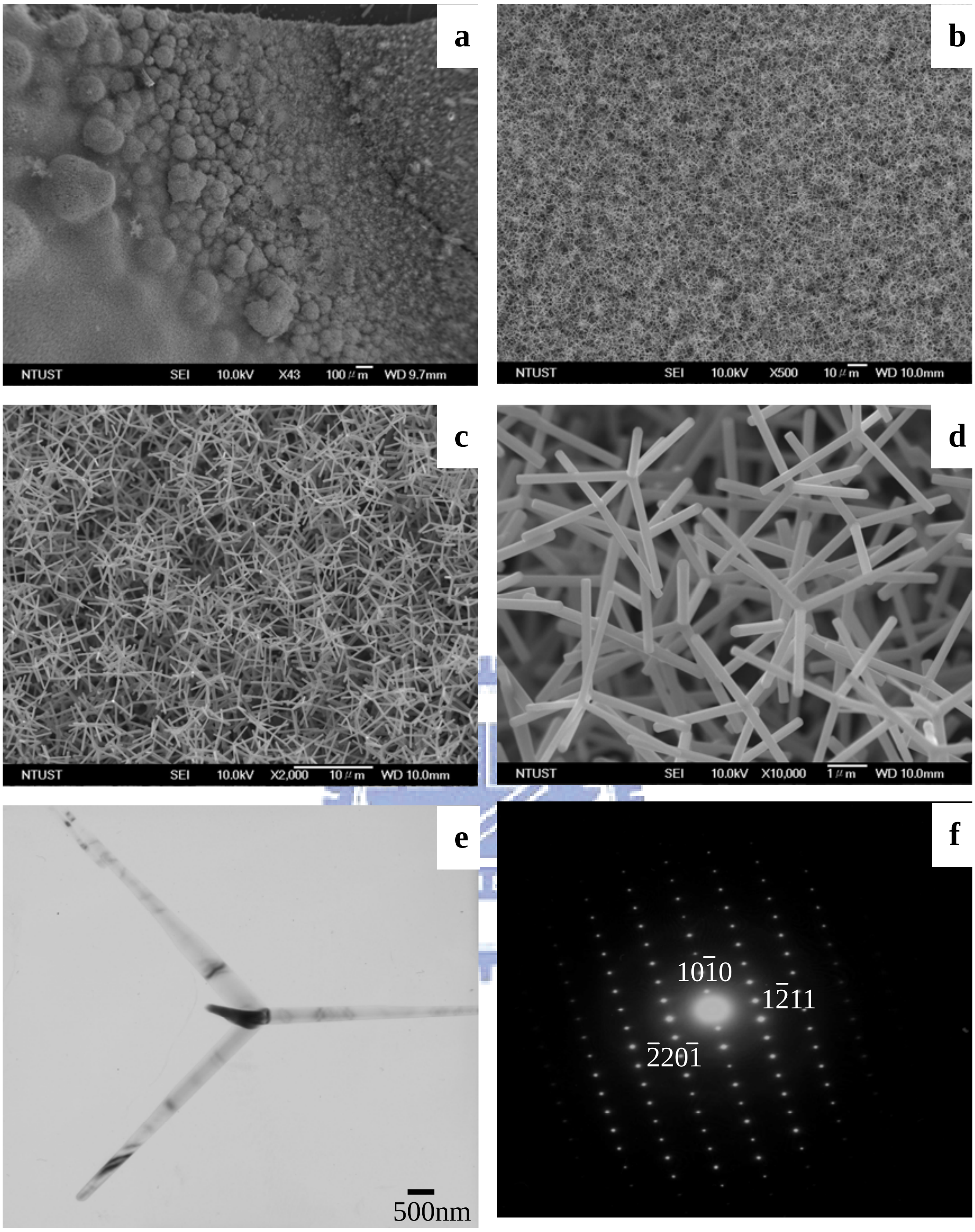

Figure 4.4 Micrographs of ZnO tetrapods grown on AAM substrate by vapor-phase-deposition at 950°C for 10min in H_2O atmosphere. **a**) Low magnification, tilted view image of sample. **b**) Face-on view image of aggregated ZnO tetrapods. **c**) The aggregated ZnO tetrapods. **d**) High magnification, face-on view of ZnO tetrapods. **e**) A bright-field TEM image of single T-ZnO nanorod. **f**) A $[\bar{1}2\bar{1}6]$ zone-axis diffraction pattern of Fig. 4.4**e**.

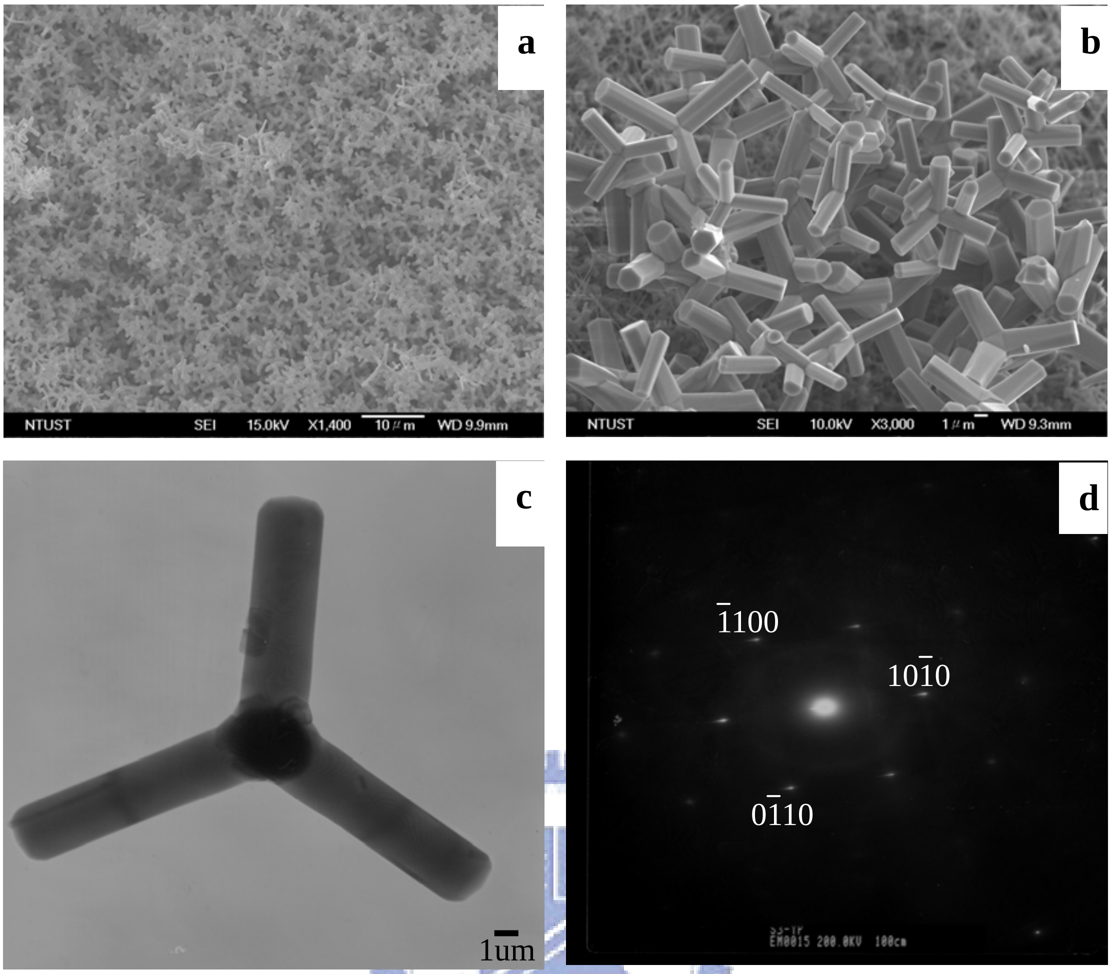

Figure 4.5 ZnO nanostructures grown on silicon substrate by vapor-phase-deposition at 950^{o}C for 10min in H_2O atmosphere. **a**) Low magnification, face-on view image of aggregated ZnO tetrapods. **b**) High magnification, armor-unit-shape ZnO tetrapods. **c**) A bright-field TEM image of single ZnO tetrapods. **d**) A [0001] zone-axis selected-area electron diffraction pattern of Fig. 4.5**c**.

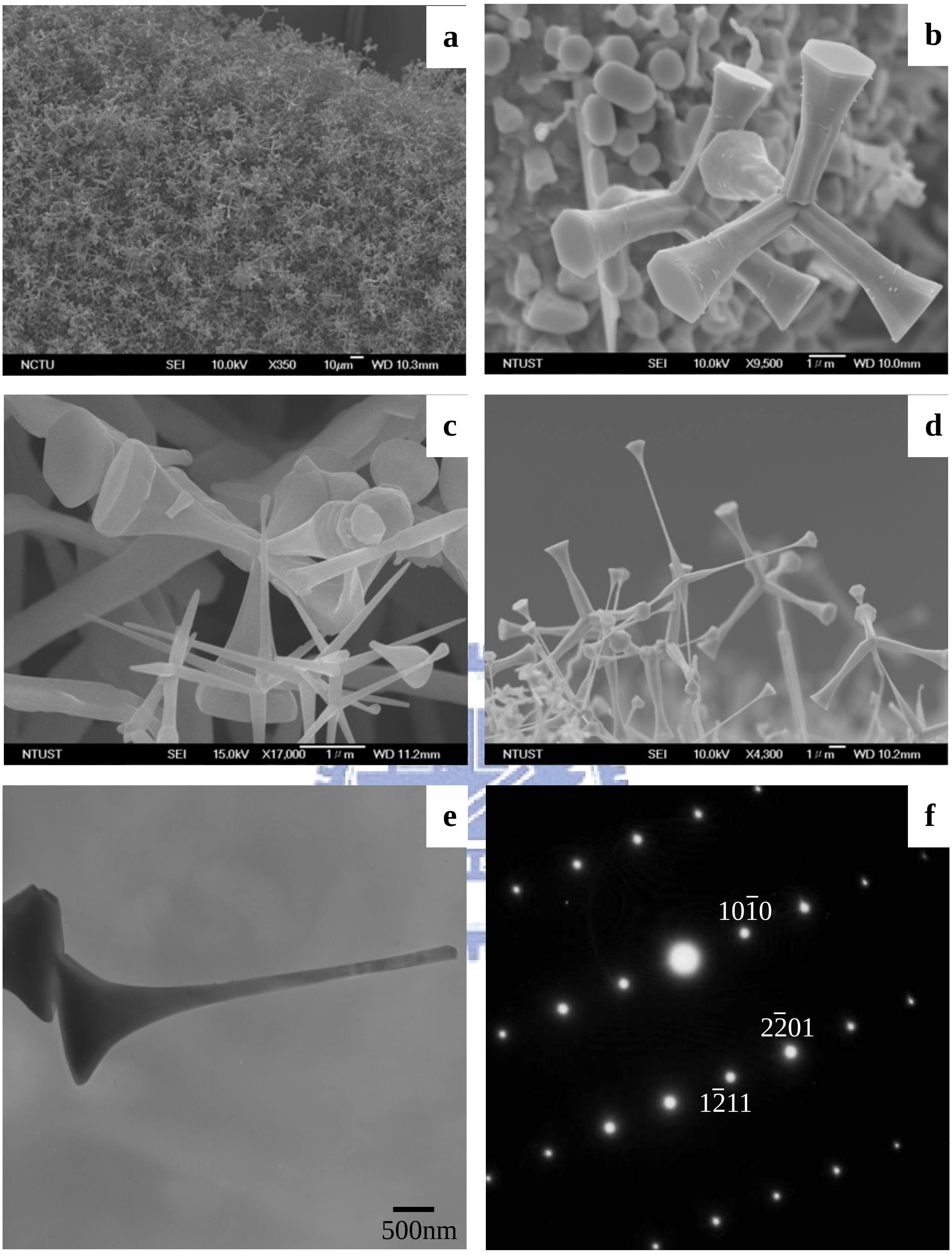

Figure 4.6 Micrographs of T-ZnO nanorods grown on silicon substrate by vapor-phase-deposition at 950°C for 10min in H_2O_2 atmosphere. **a**) Low magnification, aggregated ZnO tetrapods. **b**) Coarser trumpet-shape ZnO tetrapods. **c**) Trumpet-shape ZnO tetrapod. **d**) Finer trumpet-shape ZnO tetrapods. **e**) A bright-field TEM image of single trumpet-shape ZnO nanorod. **f**) A $[\bar{1}2\bar{1}6]$ zone-axis selected-area electron diffraction (SAED) pattern of Fig. 4.6**e**.